J. Fluid Mech. (2011), *vol.* 687, *pp.* 360–375.
doi:10.1017/jfm.2011.358

On the lift and drag of cavitating profiles and the maximum lift and drag

Dmitri V. Maklakov†

Chebotarev Institute of Mathematics and Mechanics, Kazan Federal University, Nuzhina, 17, Kazan, 420008, Russia

(Received 16 February 2011; revised 7 July 2011; accepted 24 August 2011; first published online 11 October 2011)

In this paper, on the basis of the classical Levi-Civita formulae for hydrodynamic forces exerted on any profile in an infinite cavity flow, we deduce new representations for the lift and drag. In these representations the forces are expressed only in terms of the velocity distribution along the profile surface. So, the representations are analogous to the well-known Kutta–Joukowskii theorem. By means of the new representations we find optimum velocity distributions which provide the maximum lift or maximum drag of cavitating profiles and determine corresponding optimum shapes.

Key words: jets, separated flows, wakes

1. Introduction

One of the main characteristics of the cavity flows is the cavitation number

$$Q = \frac{p_\infty - p_0}{\rho v_\infty^2/2} = \frac{v_0^2}{v_\infty^2} - 1, \tag{1.1}$$

where p_∞ and v_∞ are the pressure and stream velocity at infinity, ρ is the constant density of the fluid, p_0 is the constant pressure inside the cavity, and v_0 is the fluid velocity on the cavity boundaries. As the cavity number decreases, the length and the width of the cavity grow infinitely and the flow approaches the Helmholtz–Kirchhoff flow, in which the cavity is infinitely long, $Q = 0$, $p_0 = p_\infty$ and $v_0 = v_\infty$.

Consider a profile in the Helmholtz–Kirchhoff flow (see figure 1*a*). The flow is assumed to be steady, incompressible and irrotational. Let A and B be the points of detachment, and let O be the stagnation point. Elegant formulae for the lift and drag forces were deduced by Levi-Civita (1907). Levi-Civita mapped conformally the flow region in the physical plane $z = x + \mathrm{i}y$ onto the upper semi-circle in the parametric plane $t = \xi + \mathrm{i}\eta$(figure 1*b*), and introduced the complex potential $w = \varphi + \mathrm{i}\psi$ and the logarithmic hodograph variable

$$\omega = \mathrm{i}\log\frac{\mathrm{d}w}{v_0\,\mathrm{d}z} = \theta + \mathrm{i}\log\frac{v}{v_0}, \tag{1.2}$$

where θ is the inclination of velocity vector and v is the magnitude of velocity. Since the boundary of the flow region transforms onto the slit along the positive φ-axis in

† Email address for correspondence: dmitri.maklakov@ksu.ru

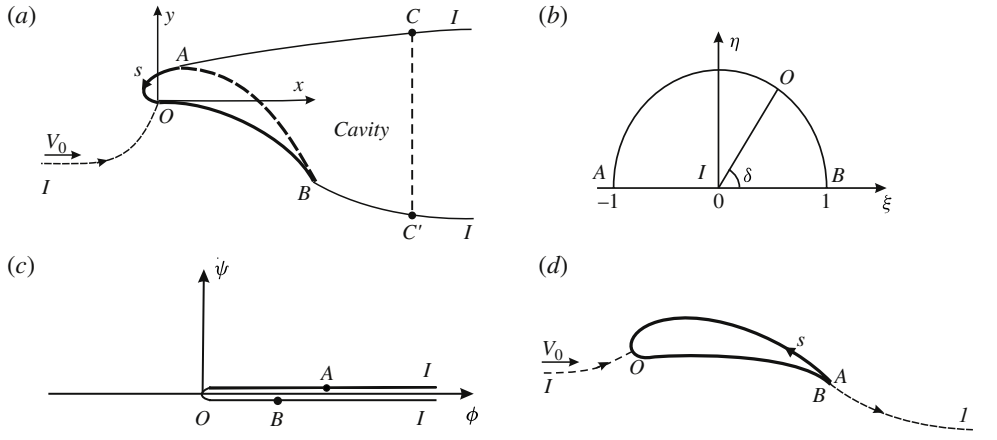

FIGURE 1. (*a*) Infinite cavity flow in the physical z-plane, (*b*) parametric t-plane, (*c*) w-plane of the complex potential, (*d*) continuous flow over an aerofoil.

the w-plane (see figure 1*c*), the conformal mapping of the t-plane onto the w-plane is

$$w(t) = \varphi_0 \left[\cos\delta - \frac{1}{2}\left(t + \frac{1}{t} \right) \right]^2, \tag{1.3}$$

where φ_0 is a positive constant which has the dimension of the velocity potential and $e^{i\delta}$ is the image of the stagnation point O in the t-plane. The Levi-Civita (1907) formulae for the lift L and drag D are as follows (see also Gilbarg 1960; Milne-Thomson 1962):

$$L = \tfrac{1}{4}\rho v_0 \varphi_0 \pi \left[4\omega'(0)\cos\delta - \omega''(0) \right], \quad D = \tfrac{1}{4}\rho v_0 \varphi_0 \pi \left[\omega'(0) \right]^2. \tag{1.4}$$

As one can see, the right-hand sides of (1.4) depend on mathematical parameters, whose physical sense is not clear. Other representations for the lift and drag are connected with the asymptotic behaviour of the cavity at infinity (see e.g. Birkhoff & Zarantonello 1957; Wu 1972):

$$y - y_0 \sim \pm C_1 x^{1/2} - C_2 \log x + O(x^{-1/2}\log x), \tag{1.5}$$

where C_1, C_2, and y_0 are constants depending on the body shape, the $\pm$ signs referring to the upper and lower free streamlines respectively. The coefficients C_1 and C_2 are related to the lift L and drag D by the equations

$$L = 2\pi\rho v_0^2 C_2, \quad D = \frac{\pi}{4}\rho v_0^2 C_1^2. \tag{1.6}$$

The formula for the lift can be formally reduced to the Kutta–Joukowskii theorem, $L = -\rho v_0 \Gamma$, where the circulation Γ should be computed in a somewhat artificial manner, namely, $\Gamma = -(C_2 v_0/2\pi)$ is the circulation calculated round the closed contour $CAOBC'C$ under the assumptions that inside the cavity the velocity is zero and the points C, C', lying on the free streamlines AI and BI, have the same abscissa, which tends to infinity (see Taylor 1926; Golubev 1949). Lavrentiev (1938) made use of the second formula to determine the shape of minimum drag in the cavity flow for a two-dimensional symmetrical body that is constrained to lie within a given rectangle.

In this paper we reduce the Levi-Civita formulae (1.4) to a physically relevant form:

$$L = \rho v_0 \int_0^l \log \frac{v_0}{v} (\boldsymbol{v} \cdot \boldsymbol{e})\, \mathrm{d}s, \quad D = \frac{\rho v_0}{4\pi} \left(\int_0^l \log \frac{v_0}{v} \frac{v}{\sqrt{\varphi}}\, \mathrm{d}s \right)^2. \tag{1.7}$$

Here l is the total wetted arc-length of the profile (the length of the curve AOB), $(\boldsymbol{v} \cdot \boldsymbol{e})$ is the dot product of the velocity vector $\boldsymbol{v} = \boldsymbol{v}(s)$ and the tangential unit vector $\boldsymbol{e} = \boldsymbol{e}(s)$ at the point on the profile surface with the arc abscissa s, reckoned from the detachment point A, $v = v(s) = |\boldsymbol{v}(s)|$ and $\varphi = \varphi(s)$ are the distributions of velocity and potential along AOB, respectively. Therefore,

$$\left.\begin{aligned} (\boldsymbol{v} \cdot \boldsymbol{e}) &= -v(s), \qquad \varphi = \int_s^{l_1} v(s)\, \mathrm{d}s \quad \text{on } AO, \\ (\boldsymbol{v} \cdot \boldsymbol{e}) &= v(s), \qquad \varphi = \int_{l_1}^{s} v(s)\, \mathrm{d}s \quad \text{on } OB, \end{aligned}\right\} \tag{1.8}$$

where l_1 is the arc abscissa of the point O.

One can see from (1.7) and (1.8) that to compute the lift and drag one needs only to know the velocity distribution $v(s)$ along the wetted part of the profile and the arc abscissa l_1 of the critical point O. Let us compare (1.7) and the well-known Kutta–Joukowskii theorem for the lift force L of an aerofoil in a continuous flow of an ideal incompressible fluid (see figure 1*d*). The theorem states that

$$L = -\rho v_0 \int_0^l (\boldsymbol{v} \cdot \boldsymbol{e})\, \mathrm{d}s, \tag{1.9}$$

where l is the perimeter of the profile contour and integration is in the same direction as in (1.7). The only difference between (1.7) and (1.9) is that in (1.7) there is a complementary dimensionless factor $\log v_0/v$ and the signs in the formulae are opposite. Some consequences of this difference will be discussed later.

As an application of (1.7) we find the velocity distributions which provide either the maximum lift or the maximum drag under the assumption that the flow satisfies the Brillouin condition: the maximum flow speed is achieved on the free boundary, i.e. $v \leqslant v_0$ (see Brillouin 1911; Birkhoff & Zarantonello 1957; Gilbarg 1960). So, we establish the exact upper bounds for the lift and drag coefficients C_L and C_D:

$$C_L \leqslant \frac{2}{\mathrm{e}} \approx 0.735759, \quad C_D \leqslant \frac{8}{\pi \mathrm{e}} \approx 0.936797. \tag{1.10}$$

Here L and D are non-dimensionalized by the total wetted arc-length l:

$$C_L = \frac{2L}{\rho v_0^2 l}, \quad C_D = \frac{2D}{\rho v_0^2 l}. \tag{1.11}$$

Making use of the obtained optimal velocity distribution for the lift, we determine a series of profile shapes with the lift coefficients which are almost equal to 2/e.

As regards the inequality for C_D in (1.10), it was first obtained by Maklakov (1988), but only for symmetric profiles (see also Maklakov 1997, 2004; Elizarov, Kasimov & Maklakov 2008). If we consider the cavity as a wake model behind a bluff body, then the optimum shape, whose drag coefficient equals the right-hand side of the inequality, can be treated as that of an ideal impermeable parachute. As a particular case of more general estimates for more complex problems, the inequality appeared in Maklakov & Uglov (1995) and Maklakov, Elizarov & Sharipov (2007), but again only

for symmetric flows. In this paper the simplicity of the second formula in (1.7) makes it possible to prove the estimate for any profile.

We should note that in spite of the fact that we seek optimal shapes for the case $Q = 0$, the shapes should remain approximately optimal for $Q > 0$, since the rule

$$C_L(Q) \approx C_L(0)(1 + Q), \quad C_D(Q) \approx C_D(0)(1 + Q) \tag{1.12}$$

is known to relate approximately the lift and drag coefficients C_L and C_D at $Q = 0$ to the lift and drag coefficients of the same body for $Q > 0$ (see e.g. Franc & Michel 2004). In particular, Maklakov & Uglov (1995) demonstrated that in the range $0 \leqslant Q \leqslant 2$ the shapes of maximum drag are practically independent of Q, hence the optimum shape at $Q = 0$ turns out to be universal. The recalculation rule is based on the fact that the ratio v/v_0 on the profile surface only slightly depends on Q.

2. Analogues of the Kutta–Joukowskii theorem for the infinite cavity model

Consider the Levi-Civita function $\omega(t)$ defined by (1.2). Since $v = v_0$ on the free streamlines AI and BI, the function $\omega(t)$ satisfies the boundary condition

$$\operatorname{Im}\omega(\xi) = 0, \quad -1 \leqslant \xi \leqslant 1. \tag{2.1}$$

We introduce the function

$$\nu(\gamma) = \log\frac{v_0}{v(\gamma)} = -\operatorname{Im}\omega(\mathrm{e}^{\mathrm{i}\gamma}), \quad 0 \leqslant \gamma \leqslant \pi, \tag{2.2}$$

where γ is the polar angle in the parametric t-plane. Let $\Omega(t) = \mathrm{i}\omega(t)$. Then

$$\operatorname{Re}\Omega(\mathrm{e}^{\mathrm{i}\gamma}) = \nu(\gamma) \quad \text{for } 0 \leqslant \gamma \leqslant \pi, \quad \operatorname{Re}\Omega(\xi) = 0 \quad \text{for } -1 \leqslant \xi \leqslant 1. \tag{2.3}$$

The second boundary condition in (2.3) allows us to continue analytically the function $\Omega(t)$ across the real segment $[-1, 1]$ from the upper semi-circle onto the entire unit disk, the real part of $\Omega(\mathrm{e}^{\mathrm{i}\gamma})$, equal to $\nu(\gamma)$, being an odd function for $\gamma \in [-\pi, \pi]$. With the Schwarz–Poisson formula we find $\Omega(t)$, and after this $\omega(t) = -\mathrm{i}\Omega(t)$:

$$\omega(t) = -\frac{2t}{\pi}\int_0^\pi \frac{\nu(\gamma)\sin(\gamma)\,\mathrm{d}\gamma}{t^2 - 2t\cos\gamma + 1}. \tag{2.4}$$

Straightforward computations give

$$\omega'(0) = -\frac{2}{\pi}\int_0^\pi \nu(\gamma)\sin\gamma\,\mathrm{d}\gamma, \quad \omega''(0) = -\frac{4}{\pi}\int_0^\pi \nu(\gamma)\sin 2\gamma\,\mathrm{d}\gamma. \tag{2.5}$$

We insert these derivatives into the Levi-Civita formulae (1.4) for the lift to get

$$L = 2\rho v_0\varphi\int_0^\pi \nu(\gamma)\sin\gamma(\cos\gamma - \cos\delta)\,\mathrm{d}\gamma. \tag{2.6}$$

By means of (1.3) we find on the parametric circumference

$$\varphi(\gamma) = \varphi_0(\cos\delta - \cos\gamma)^2 \quad \text{and} \quad \varphi'(\gamma) = -2\varphi_0\sin\gamma(\cos\gamma - \cos\delta). \tag{2.7}$$

Comparison of (2.6) and the second formula in (2.7) yields

$$L = -\rho v_0\int_0^\pi \nu(\gamma)\frac{\mathrm{d}\varphi}{\mathrm{d}\gamma}\,\mathrm{d}\gamma = \rho v_0\int_\pi^0 \nu(\gamma)\frac{\mathrm{d}\varphi}{\mathrm{d}\gamma}\,\mathrm{d}\gamma = \rho v_0\int_\pi^0 \nu(\gamma)\,\mathrm{d}\varphi. \tag{2.8}$$

Now we pass to integration in the physical plane. Taking into account that $\mathrm{d}\varphi = (\boldsymbol{v}\cdot\boldsymbol{e})\,\mathrm{d}s$ and $\nu = \log v_0/v$, we come to the first formula in (1.7).

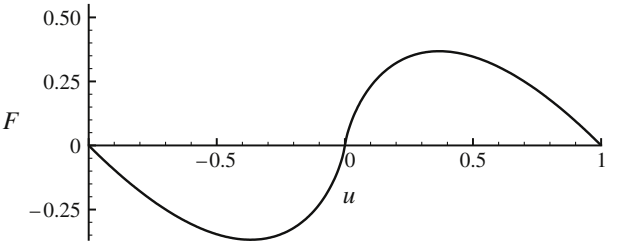

FIGURE 2. The graph of the function $F(u)$.

To deduce the second formula in (1.7) we need to express $\omega'(0)$ in terms of $v(s)$. To do so we write the first formula in (2.5) as follows:

$$\omega'(0) = \frac{2}{\pi}\int_0^{\pi} v(\gamma)\,\mathrm{d}\cos\gamma. \tag{2.9}$$

From the first formula in (2.7) we conclude that

$$\cos\gamma = \begin{cases} \sqrt{\varphi/\varphi_0} + \cos\delta & \text{for } 0 < \gamma < \delta, \\ -\sqrt{\varphi/\varphi_0} + \cos\delta & \text{for } \delta < \gamma < \pi. \end{cases} \tag{2.10}$$

Substituting $\cos\gamma$ into (2.9) yields

$$\omega'(0) = \frac{1}{\pi\sqrt{\varphi_0}}\left(\int_0^{\delta} \frac{v(\gamma)\,\mathrm{d}\varphi}{\sqrt{\varphi}} - \int_{\delta}^{\pi} \frac{v(\gamma)\,\mathrm{d}\varphi}{\sqrt{\varphi}}\right). \tag{2.11}$$

Passing to integration in the physical z-plane and taking into account that $\mathrm{d}\varphi = -v\,\mathrm{d}s$ on AO and $\mathrm{d}\varphi = v\,\mathrm{d}s$ on OB, we conclude that

$$\omega'(0) = -\frac{1}{\pi\sqrt{\varphi_0}}\int_0^{l} \log\frac{v_0}{v}\frac{v\,\mathrm{d}s}{\sqrt{\varphi}}. \tag{2.12}$$

Inserting this expression into the second formula in (1.4), we prove the second formula in (1.7).

3. Upper estimate for the lift

The class of profiles in which we shall seek the profile of maximum lift is described by the following two conditions. (i) The profiles have a fixed wetted arc-length l. (ii) The cavity flows over them satisfy the Brillouin condition: the maximum flow speed is achieved on the free boundary, i.e. $v \leqslant v_0$.

To find the optimal velocity distribution we introduce the function $u(s) = (\boldsymbol{v}\cdot\boldsymbol{e})/v_0$. Then $|u(s)| \leqslant 1$, $u(s) > 0$ on OB, $u(s) < 0$ on AO, and formula (1.7) can be rewritten as

$$L = \rho v_0^2 \int_0^{l} F[u(s)]\,\mathrm{d}s, \quad F(u) = -u\log|u|. \tag{3.1}$$

The graph of the function $F(u)$ is shown in figure 2. On the segment $[-1, 1]$ the function has the only maximum at the point $u = \mathrm{e}^{-1}$ and the value of this maximum $F_{max} = \mathrm{e}^{-1}$. Now we can estimate the integral in (3.1). Substituting $F_{max} = 1/\mathrm{e}$ for the integrand in (3.1), we obtain that $L \leqslant \rho v_0^2/\mathrm{e}$, hence the first estimate in (1.10) is true. The equality in the estimate is only possible if $u(s) = \mathrm{e}^{-1}$. Since for the optimum

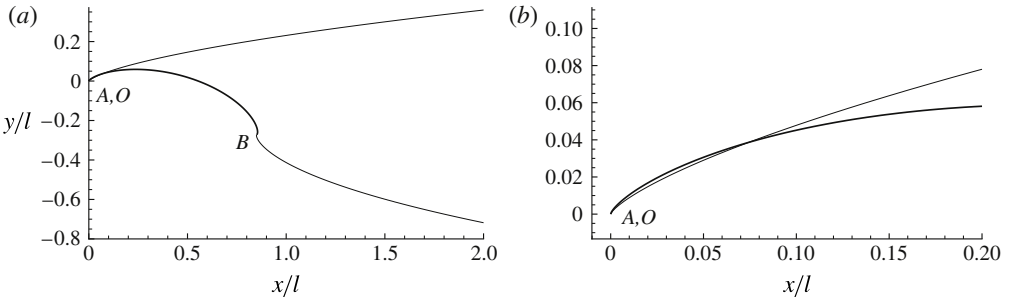

FIGURE 3. (*a*) Shape of the optimum profile and free streamlines. (*b*) Magnification of the shape near the point *A*.

profile $u(s) > 0$ everywhere, the part AO of the profile disappears ($l_1 = 0$), the points A and O coincide and the parameter $\delta = \pi$.

At maximum lift we have $u(s) = \mathrm{e}^{-1}$, hence the velocity distribution along the optimal profile is given by the equation

$$v(s) = \mathrm{e}^{-1} v_0 = \text{const.}, \quad 0 \leqslant s \leqslant l. \tag{3.2}$$

From (2.2) and (3.2) we conclude that

$$\nu(\gamma) = 1, \quad 0 \leqslant \gamma \leqslant \pi. \tag{3.3}$$

Knowing the function $\nu(\gamma)$ and the parameter δ, we can easily obtain analytical representations for the shape of the profile and free streamlines. We will derive these representations in the following section and right now we demonstrate the shape in figure 3(*a*,*b*). As one can see from figure 3(*b*) the result is rather discouraging, since in the neighbourhood of the point A the free surface AI intersects the profile. So, in this neighbourhood the flow domain is two-sheeted.

It is evident why the segment AO disappears for the optimum profile. Indeed, according to (1.7) the contribution of the segment AO to the lift is negative (under the Brillouin condition the factor $\log v_0/v$ is positive), whereas the contribution of OB is positive. So to increase the lift the above procedure of optimization removes the segment with the negative contribution. But it seems the presence of the segment AO is of importance to obtaining an one-sheeted flow domain. In the Appendix we prove the following theorem.

THEOREM 1. *If a curve AB is everywhere convex or everywhere concave, has a finite curvature, which does not vanish identically, and the curve is located in an infinite cavity flow so that the critical point O coincides with the end point A , then the flow domain is two-sheeted.*

The theorem demonstrates that this useless (from the point of view of maximizing the lift) segment OA is necessary to obtain a realistic one-sheeted flow.

4. Modified profiles with lift almost equal to maximum

The goal of this section is to design profiles which have lift almost equal to maximum, with the flow domain over them to be one-sheeted. Hereafter it is more convenient to measure the arc abscissa s not from the point A but from the point O, so that the direction of increase of s coincides with that of the potential φ. Thus the s

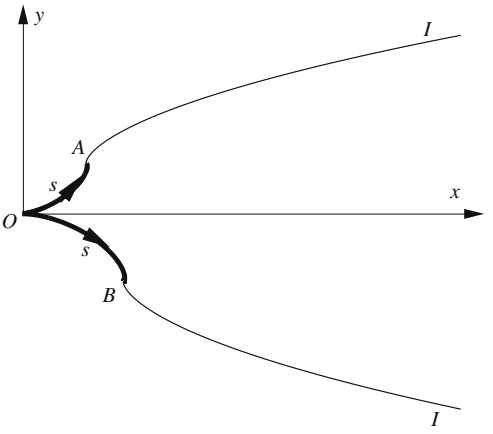

FIGURE 4. Scheme of the cavity flow over a modified profile.

is always positive and every fixed s defines two points on the boundary of the flow: one point on the curve OAI and another on the curve OBI. For this s we always have $\mathrm{d}\varphi/\mathrm{d}s = v(s)$. The previous system of reckoning s was convenient for writing the formulae (1.7) compactly.

Let us introduce two dimensionless functions $u_1(\sigma)$ and $u_2(\sigma)$, $0 \leqslant \sigma \leqslant 1$, such that

$$\frac{v}{v_0} = \begin{cases} u_1(s/l_1) & \text{on } OA, \\ u_2(s/l_2) & \text{on } OB, \end{cases} \tag{4.1}$$

where $l_2 = l - l_1$ is the length of the segment OB. The functions $u_1(\sigma)$ and $u_2(\sigma)$ are non-negative. If the curves OA and OB are smooth, then these functions are strictly positive everywhere except possibly the point $\sigma = 0$, where they can vanish. Under the Brillouin condition they satisfy the inequalities $u_1(\sigma) \leqslant 1$, $u_2(\sigma) \leqslant 1$. In terms of $u_1(\sigma)$ and $u_2(\sigma)$ the formulae (1.7) can be rewritten as

$$L = \rho v_0^2 l\{(1-\varepsilon)I[u_2] - \varepsilon I[u_1]\}, \quad D = \frac{\rho v_0^2 l}{4\pi}\left\{\sqrt{\varepsilon}J[u_1] + \sqrt{1-\varepsilon}J[u_2]\right\}^2, \tag{4.2}$$

where $\varepsilon = l_1/l$, and $I[u]$ and $J[u]$ are nonlinear functionals defined as follows:

$$I[u] = -\int_0^1 u(\sigma)\log u(\sigma)\,\mathrm{d}\sigma, \quad J[u] = -\int_0^1 \frac{u(\sigma)\log u(\sigma)\,\mathrm{d}\sigma}{\sqrt{\int_0^\sigma u(\sigma_1)\,\mathrm{d}\sigma_1}}. \tag{4.3}$$

As one can see from (4.3), under the Brillouin condition the values of the functional $J[u]$ at $u = u_1$ and $u = u_2$ are non-negative, and therefore both segments OA and OB give positive contributions to the drag.

To design a profile with the lift almost equal to maximum we proceed in the simplest manner. We set $v(s) = \mathrm{e}^{-1}v_0 = \text{const.}$, as in the case of the optimum profile, but we introduce the segment OA with the arc-length $l_1 \neq 0$. Since $v(s) = \mathrm{e}^{-1}v_0 = \text{const.}$, and nowhere vanishes on the profile surface, the critical point O is a cusp (see figure 4).

For the case $v(s) = \mathrm{e}^{-1}v_0$ we have $u_1(\sigma) = u_2(\sigma) = \mathrm{e}^{-1}$, and straightforward computations by the formulae (4.2) lead us to the equations

$$C_L = \frac{2}{\mathrm{e}}(1-2\varepsilon), \quad C_D = \frac{2p^2}{\pi\mathrm{e}}, \quad \text{where } p = \sqrt{\varepsilon} + \sqrt{1-\varepsilon}, \tag{4.4}$$

and ε will be taken to be small subsequently.

So, introducing the segment OA decreases the lift coefficient C_L by a factor of $1-2\varepsilon$ and increases the drag coefficient C_D by a factor of $p^2 = 1 + 2\sqrt{\varepsilon(1-\varepsilon)}$. For the profile of maximum lift at $\varepsilon = 0$, the drag coefficient $C_D = 2/(\pi\mathrm{e})$.

Note also that we computed these coefficients before solving the hydrodynamic problem and finding any mathematical parameters inherent to the Levi-Civita parametrization. But to define the shape of the profile and free boundaries these parameters are certainly necessary. So we need to determine φ_0, δ and $\omega(t)$.

Let us denote by φ_A and φ_B the values of the potential at the points A and B respectively. Then

$$\varphi_A = v_0 l_1 \int_0^1 u_1(\sigma)\,\mathrm{d}\sigma, \quad \varphi_B = v_0 l_2 \int_0^1 u_2(\sigma)\,\mathrm{d}\sigma. \tag{4.5}$$

From (1.3) we infer

$$\sqrt{\varphi_A} = \sqrt{\varphi_0}(1+\cos\delta), \quad \sqrt{\varphi_B} = \sqrt{\varphi_0}(1-\cos\delta). \tag{4.6}$$

It follows from these equations that

$$\varphi_0 = \frac{1}{4}\left(\sqrt{\varphi_A} + \sqrt{\varphi_B}\right)^2, \quad \delta = 2\arctan\sqrt[4]{\frac{\varphi_B}{\varphi_A}}. \tag{4.7}$$

In our case, when $u_1(\sigma) = u_2(\sigma) = \mathrm{e}^{-1}$, we have $\varphi_A = v_0 l \mathrm{e}^{-1}\varepsilon$, $\varphi_B = v_0 l \mathrm{e}^{-1}(1-\varepsilon)$,

$$\varphi_0 = \frac{v_0 l}{4\mathrm{e}}p^2, \quad \delta = 2\arctan\sqrt[4]{\frac{1-\varepsilon}{\varepsilon}}, \tag{4.8}$$

where p is defined in (4.4).

Earlier we deduced from (2.2) and (3.2) that for the profile of maximum lift the function, $\nu(\gamma) = 1$. Since $v(s) = \mathrm{e}^{-1}v_0 = \text{const.}$, the function $\nu(\gamma)$ remains the same as earlier. Substituting $\nu(\gamma) = 1$ into (2.4), we get

$$\omega(t) = -\frac{2}{\pi}\log\frac{1+t}{1-t}. \tag{4.9}$$

Now we know all parameters and functions of the Levi-Civita parametrization and, in principle, we are able to determine the desired flow domain in the ordinary way, namely, by integrating the function

$$\frac{\mathrm{d}z}{\mathrm{d}t} = \frac{\mathrm{d}z}{\mathrm{d}w}\frac{\mathrm{d}w}{\mathrm{d}t} = \frac{\varphi_0}{2v_0}\frac{(t^2-1)(t^2-2t\cos\delta+1)}{t^3}\mathrm{e}^{\mathrm{i}\omega(t)}. \tag{4.10}$$

Here we proceed in more explicit manner, namely, we find analytically the function $\theta(s)$ for the curves OAI and OBI. Then the boundaries of the flow region can be determined by the simple parametric equations

$$x(s) = \int_0^s \cos\theta(s_1)\,\mathrm{d}s_1, \quad y(s) = \int_0^s \sin\theta(s_1)\,\mathrm{d}s_1, \tag{4.11}$$

and the formulae are correct for both OAI and OBI.

To find explicitly $\theta(s)$ we introduce a new complex parametric variable

$$q = -\frac{(1+t)^2}{4t}, \tag{4.12}$$

which changes in the upper half-plane. It is easy to see from (1.3) that the complex potential

$$w = 4\varphi_0\left(\cos^2\frac{\delta}{2} + q\right)^2, \tag{4.13}$$

and hence

$$q = \pm\frac{1}{2}\sqrt{\frac{\varphi}{\varphi_0}} - \cos^2\frac{\delta}{2}, \tag{4.14}$$

where the signs + and − correspond to the curve OAI and OBI, respectively.

On the other hand we can compute the distribution of the potential φ along the boundary of the flow:

$$\varphi = \begin{cases} \mathrm{e}^{-1}v_0 l(s/l) & \text{on } OA \text{ and } OB, \\ v_0 l(s/l-\varepsilon) + \varphi_A & \text{on } AI, \\ v_0 l(s/l-1+\varepsilon) + \varphi_B & \text{on } BI, \end{cases} \tag{4.15}$$

Inserting (4.15) into (4.14) we find

$$q(s) = \begin{cases} \dfrac{1}{p}(\sqrt{s/l} - \sqrt{\varepsilon}) & 0 \leqslant s/l \leqslant \varepsilon \text{ on } OA, \\ \dfrac{1}{p}(\sqrt{\mathrm{e}(s/l-\varepsilon)+\varepsilon} - \sqrt{\varepsilon}) & s/l > \varepsilon \text{ on } AI, \\ -\dfrac{1}{p}(\sqrt{s/l} + \sqrt{\varepsilon}) & 0 \leqslant s/l \leqslant 1-\varepsilon \text{ on } OB, \\ -\dfrac{1}{p}(\sqrt{\mathrm{e}(s/l+\varepsilon-1)+1-\varepsilon} + \sqrt{\varepsilon}) & s/l > 1-\varepsilon \text{ on } BI, \end{cases} \tag{4.16}$$

where p is defined in (4.4), and we take into account that $\cos^2(\delta/2) = \sqrt{\varepsilon}/p$.

In terms of q the function $\omega(t)$ takes the form

$$\omega(t) = \frac{1}{\pi}\log\frac{1+q}{q}. \tag{4.17}$$

Hence

$$\theta = \frac{1}{\pi}\log\left|\frac{1+q(s)}{q(s)}\right|. \tag{4.18}$$

So, (4.16) and (4.18) define in an explicit analytical form the function $\theta(s)$ on the boundaries of the flow. At $\varepsilon = 0$ we obtain $\theta(s)$ for the two-sheeted flow shown in figure 3.

In figure 5 we demonstrate the shapes of modified profiles which create lift very close to maximum. As one can see, starting with $\varepsilon = 0.0005$, the flow region is one-sheeted in the neighbourhood of the leading edge O. Inclusion of the small curvilinear segment OA prevents overlapping of the upper free streamline with the profile. The constant velocity $v = v_0\mathrm{e}^{-1}$ along the profile surface creates curious dolphin-nose

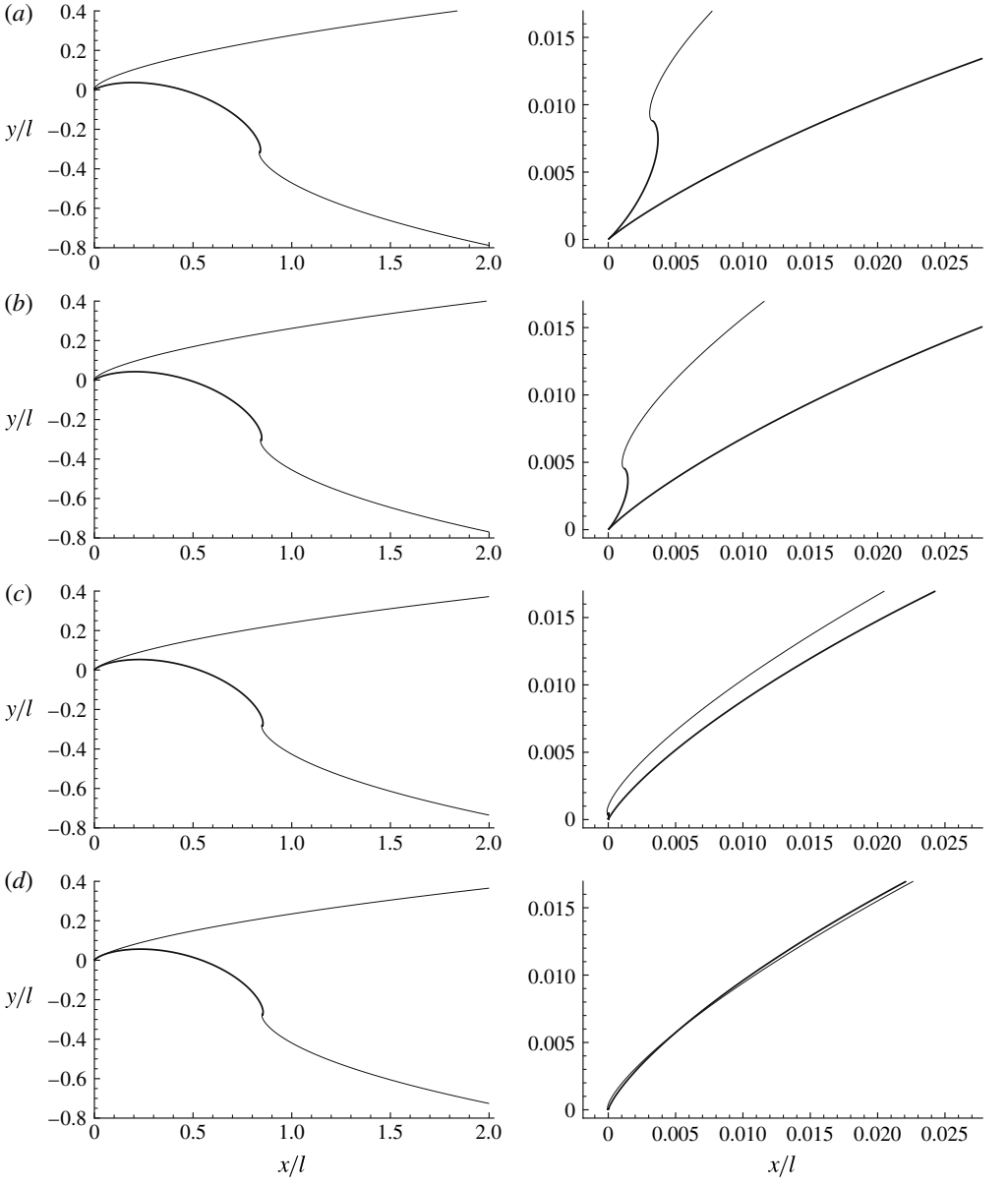

FIGURE 5. Shapes of dolphin-nose profiles and free streamlines: (*a*) $\varepsilon = 0.01$, (*b*) $\varepsilon = 0.005$, (*c*) $\varepsilon = 0.0005$, (*d*) $\varepsilon = 0.0001$. The figures on the right are magnifications of the figures on the left near the point O.

shapes in the flow boundary near the leading edge O. The two-sheeted flow appears only at $\varepsilon = 0.0001$. The lifts of the profiles in figure 5(*a–c*) differ from the maximum lift only by 2 %, 1 % and 0.1 % respectively.

Note that the boundaries of the flow in figure 4 have been obtained by the formulae (4.16) and (4.18) at $\varepsilon = 0.4$.

One can see from (4.16) and (4.18) that $\theta(s) \to +\infty$ as $s/l \pm 0 \to \varepsilon$ on the boundary OAI and $\theta(s) \to -\infty$ as $s/l \pm 0 \to 1 - \varepsilon$ on the boundary OBI. This means that

near the end points A and B the boundary of the flow region contains four infinitely rolled-up spiral curves, one pair of spirals near the point A and another pair near the point B. The reason these spirals appear is the jump of the velocity at the points A and B: on the profile surface $v = v_0 e^{-1}$, whereas on the free streamlines $v = v_0$. So the flow near the points A and B is asymptotically close to a spiral flow between two free streamlines with constant but different velocities on each of them. Such flows are discussed in Birkhoff & Zarantonello (1957, figure 35).

A simple analysis of (4.16) and (4.18) shows that the spirals are asymptotically logarithmic. If we take the points A and B for the centres of the spirals and denote by r and α the polar radius and the polar angle with respect to these centres, then it is easy to deduce from (4.16) and (4.18) that the equations of the spirals have the form

$$r = C \exp(\pm \pi \alpha), \tag{4.19}$$

where C is a certain positive constant, which should be determined for each of the four spirals, and the signs $+$ and $-$ correspond to the pairs of spirals near the point B and A, respectively. Concrete values of the constants C are not of great importance and we do not give them here, but the factor π in the exponent plays a very important role. Indeed, as follows from (4.19), with every half-revolution of the polar radius r its length decreases by a factor of $e^{-\pi^2} \approx 0.5 \times 10^{-4}$. This means that the spirals cannot be seen at any scales. For instance, if we take the initial $r = 1$ m, after a half-revolution its length will be 0.05 mm, and the remaining part of the spiral will be like a point.

The spirals of this kind appeared in all previous papers, where isoperimetric optimization problems with free streamlines were solved (see Maklakov 1988, 1997, 1999, 2005; Maklakov & Uglov 1995; Maklakov *et al.* 2007; Elizarov *et al.* 2008). As was demonstrated by Maklakov (1997, 1999) and Elizarov *et al.* (2008), the contribution of these tiny spirals to the hydrodynamic forces is negligible.

We should note that in the case of non-realistic two-sheeted flow over the optimum profile ($\varepsilon = 0$), the equations of the pair of spirals near the point A, coinciding with O, have the form

$$r = C \exp(-2\pi \alpha). \tag{4.20}$$

Now the factor in the exponent is 2π, $e^{-2\pi^2} \approx 0.25 \times 10^{-8}$. Because of this the spiral leading edge in figure 3 looks like a razor blade.

5. Upper estimate for the drag

We shall seek the profile of maximum drag in the class of profiles which satisfy conditions (i) and (ii) of § 3. First we consider the case of symmetric flows over symmetric profiles. For this case $l_1 = l_2$, $\varepsilon = 1/2$, $u_1(\sigma) = u_2(\sigma) = u(\sigma)$, where $u_1(\sigma)$ and $u_2(\sigma)$ are defined in (4.1). The function $u(\sigma)$ is a non-negative function such that the functional $J[u]$ in (4.3) is finite. According to (4.2), for the drag D of the symmetric profiles we have the following formula:

$$D = \frac{\rho v_0^2 l}{2\pi} J^2[u]. \tag{5.1}$$

Under the Brillouin condition the function $u(\sigma) \leqslant 1$ and the functional $J[u]$ is non-negative. Hence, to find the maximum of D it is enough to maximize the functional $J[u]$. In Maklakov (1988) the problem of finding the symmetric profile of maximum drag has already been solved by means of Levi-Civita parametrization (see also Maklakov 1997, 2004; Elizarov *et al.* 2008). It has been established that

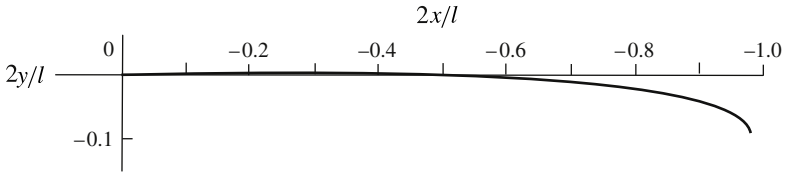

FIGURE 6. Half of the profile of maximum drag.

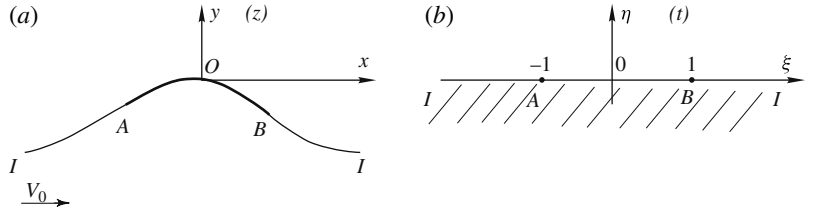

FIGURE 7. Flow region in the physical z-plane (a) and the parametric t-plane (b) for the sprayless planing surface.

under the Brillouin condition the maximum drag is achieved for the profile with the velocity distribution $v(s) = 2\mathrm{e}^{-1}s/l$. Therefore, $u(\sigma) = \mathrm{e}^{-1}\sigma$, and inserting this $u(\sigma)$ into (4.3) we find that for symmetric profiles $J_{max} = 2\sqrt{2/\mathrm{e}}$, $D_{max} = 4\rho v_0^2 l/(\pi\mathrm{e})$.

Now consider the case of an arbitrary profile. As follows from (4.2),

$$D \leqslant \frac{\rho v_0^2 l}{4\pi} J_{max}^2 \left(\sqrt{\varepsilon} + \sqrt{1-\varepsilon}\right)^2, \tag{5.2}$$

because $J[u_1] \leqslant J_{max}$ and $J[u_2] \leqslant J_{max}$. Equality in (5.2) is only possible if $u_1(\sigma) = u_1(\sigma) = \mathrm{e}^{-1}\sigma$. The function $f(\varepsilon) = \left(\sqrt{\varepsilon} + \sqrt{1-\varepsilon}\right)^2$ achieves its maximum with respect to ε at $\varepsilon = 1/2$. So, for any profile we have $D \leqslant 4\rho v_0^2 l/(\pi\mathrm{e})$, and equality is only possible if $u_1(\sigma) = u_2(\sigma) = \mathrm{e}^{-1}\sigma$, $\varepsilon = 1/2$, i.e. for the symmetric profile of maximum drag. Thus, we have proved the second estimate in (1.10).

For completeness, in figure 6 we reproduce a graph from Maklakov (1997, figure 4), with half of the symmetric profile of maximum drag. This is just the shape of an ideal impermeable parachute.

6. A note on the lift force of a sprayless planing surface

The papers by Wu & Whitney (1972) and Maklakov (1999) have studied the problem of finding the optimum profile of a two-dimensional plate that planes on a water surface without spray formation and maximizes the lift force. The scheme of the flow region and the corresponding parametric lower half-plane are demonstrated in figure 7(*a*,*b*).

Let l be the arc-length of the plate AB, and let v_0 be the velocity at infinity. Maklakov (1999) has proved that for this flow the lift coefficient

$$C_L = \frac{2L}{\rho v_0^2 l} \leqslant \frac{2}{\mathrm{e}}, \tag{6.1}$$

and equality is only possible for the profile with the constant velocity distribution on its surface: $v = v_0\mathrm{e}^{-1}$. If one compares this result with (1.10) and (3.2), one concludes

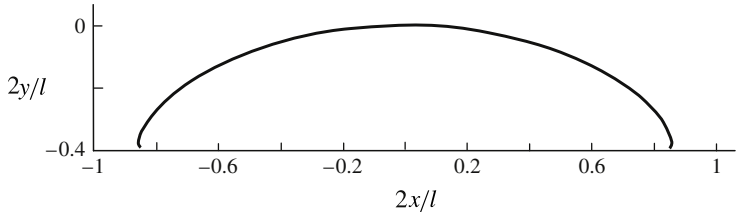

FIGURE 8. Shape of the optimum planing surface.

that, for the infinite cavity flow and for the planing surface, the upper estimates of the lift force and the optimal velocity distributions coincide.

The explanation for this curious coincidence is rather simple. Indeed, Wu & Whitney (1972) deduced the following formulae for the lift force:

$$L = \rho v_0^2 a_0 \int_{-1}^{1} \nu(\xi)\,\mathrm{d}\xi, \quad \text{where } \nu(\xi) = \log\frac{v_0}{v}, \tag{6.2}$$

and a_0 is a positive constant such that $w = a_0 v_0 t$, $w = \varphi + \mathrm{i}\psi$ being the complex potential. Now if we substitute $\mathrm{d}\xi = \mathrm{d}\varphi/(a_0 v_0)$ into (6.2), we immediately establish that the formula for the lift in (1.7), deduced for the profile in the infinite cavity flow, is also correct for the planing plate. So, for these two different types of flows the functionals for the lift forces, expressed in terms of the velocity distributions, coincide. This leads to the same estimates for the lift and the same optimum velocity distributions. But the shapes of the optimum profiles will certainly be different. For comparison we reproduce in figure 8 the optimum planing surface found in figure 3 of Maklakov (1999).

7. Conclusion

Let us assume that the flow over a cavitating profile satisfies the Brillouin condition. Then everywhere on the profile surface $v \leqslant v_0$ and the dimensionless factor $\log(v_0/v)$ in the formulae (1.7) is non-negative: $\log(v_0/v) \geqslant 0$. This means that the lower segment OB of the profile surface creates a positive contribution to the lift force, whereas the contribution of the upper segment OA is negative. For the continuous flow (figure 1*d*) we have the opposite situation, because the signs in the Kutta–Joukowskii formula and in the first formula in (1.7) are opposite. So, in the continuous flow the upper segment OA contributes to the lift with a plus sign, whereas OB does so with a minus sign. These different mechanisms of generating the lift force certainly should be taken into account in designing cavitating lifting hydrofoils. As for the drag force, according to the second formula in (1.7), both segments OA and OB give a positive contribution to the drag.

From the point of view of maximizing the lift the segment OA is useless and should be removed, but as has been demonstrated in § 3, without the segment the flow will be two-sheeted and cannot be realized. Moreover, the segment OA is necessary to obtain satisfactory strength properties of the leading edge.

Consider now any part of the segment OB. If we set $v = v_0\mathrm{e}^{-1}$ on this part, then it will give the maximum contribution to the lift, since under the Brillouin condition the integrand in the formula for the lift achieves its maximum at $v = v_0\mathrm{e}^{-1}$ (see figure 2). The dolphin-nose profiles of § 4 have been designed in just this manner, because everywhere on OB we set $v = v_0\mathrm{e}^{-1}$. But in such a design the drag force is not taken

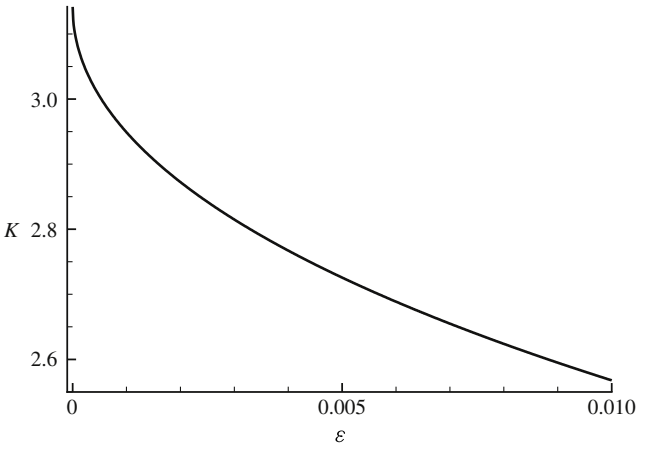

FIGURE 9. Lift-to-drag ratio K versus ε for dolphin-nose profiles.

into account. According to (4.4), the lift-to-drag ratio of these profiles is

$$K = \frac{L}{D} = \pi \frac{1 - 2\varepsilon}{(\sqrt{\varepsilon} + \sqrt{1 - \varepsilon})^2}, \tag{7.1}$$

where $\varepsilon = l_1/l$ is the dimensionless arc-length of the segment OA. In figure 9 we show the function $K(\varepsilon)$. As one can see from the figure, even for small ε we have a significant decrease in K. One possible way of avoiding this decrease is to introduce the drag force in the formulation of the optimization problem. For example, given the lift of cavitating profiles $L < \rho v_0^2/\mathrm{e}$, find the profile of minimum drag. The formulation presented here has the potential to solve this problem.

In § 6 of the paper we have shown that the first formula in (1.7) for the lift turns out to be correct not only for cavitating profiles, but for sprayless planing surfaces too. It is quite possible that there exist other free streamline flows for which this formula is true.

Appendix. Proof of the theorem in § 3

Assume that the points O and A coincide; then the point A is a cusp point. As in § 4 we measure the arc abscissa s from the point A and prescribe that s to be everywhere positive on the boundary of the flow, so again the increase of s coincides with that of the potential φ. From (1.3) at $\delta = \pi$ we infer that

$$w(t) = \varphi_0 \left[1 + \frac{1}{2}\left(t + \frac{1}{t}\right)\right]^2. \tag{A 1}$$

From this we deduce that on the real diameter

$$\frac{\mathrm{d}\varphi}{\mathrm{d}\xi} = \frac{\varphi_0}{2} \frac{(\xi - 1)(\xi + 1)^3}{\xi^3}, \quad -1 \leqslant \xi \leqslant 1, \tag{A 2}$$

and on the parametric circumference

$$\frac{\mathrm{d}\varphi}{\mathrm{d}\gamma} = -2\varphi_0 \sin\gamma(1 + \cos\gamma), \quad 0 \leqslant \gamma \leqslant \pi. \tag{A 3}$$

On the curve AB we have $(\mathrm{d}\theta/\mathrm{d}s) = (\mathrm{d}\theta/\mathrm{d}\gamma)(\mathrm{d}\gamma/\mathrm{d}\varphi)(\mathrm{d}\varphi/\mathrm{d}s)$. Hence

$$\theta'(\gamma) = -\frac{2\varphi_0 \sin\gamma(1+\cos\gamma)}{v(\gamma)}\frac{\mathrm{d}\theta}{\mathrm{d}s}. \tag{A 4}$$

On the free streamlines AI and BI we have $(\mathrm{d}\theta/\mathrm{d}s) = (\mathrm{d}\theta/\mathrm{d}\xi)(\mathrm{d}\xi/\mathrm{d}\varphi)(\mathrm{d}\varphi/\mathrm{d}s)$. Hence

$$\frac{\mathrm{d}\theta}{\mathrm{d}s} = \frac{2v_0\xi^3\theta'(\xi)}{\varphi_0(\xi-1)(\xi+1)^3}. \tag{A 5}$$

According to Gurevich (1966),

$$\omega(t) = \frac{1-t^2}{\pi}\int_0^\pi \frac{\theta(\gamma)\,\mathrm{d}\gamma}{1-2t\cos\gamma+t^2}. \tag{A 6}$$

Therefore

$$\omega'(t) = \frac{2}{\pi}\int_0^\pi \theta(\gamma)\frac{(1+t^2)\cos\gamma - 2t}{(1-2t\cos\gamma+t^2)^2}\,\mathrm{d}\gamma. \tag{A 7}$$

Integrating by parts, we find on the real diameter

$$\theta'(\xi) = -\frac{2}{\pi}\int_0^\pi \frac{\theta'(\gamma)\sin\gamma\,\mathrm{d}\gamma}{1-2\xi\cos\gamma+\xi^2}. \tag{A 8}$$

Now let us analyse the obtained formulae (A 4)–(A 8). First, we consider the case of a convex curve with curvature $\mathrm{d}\theta/\mathrm{d}s \leqslant 0$. From (A 4) we conclude that $\theta'(\gamma) \geqslant 0$ and does not vanish identically. Then it follows from (A 8) that $\theta'(\xi) > 0$ for $-1 \leqslant \xi \leqslant 1$ because

$$\frac{\sin\gamma}{1-2\xi\cos\gamma+\xi^2} > 0 \quad \text{for } -1 \leqslant \xi \leqslant 1,\ 0 < \gamma < \pi. \tag{A 9}$$

Making use of (A 5) leads us to the conclusion that on the free streamline AI we have $(\mathrm{d}\theta/\mathrm{d}s) < 0$ and

$$\lim_{s\to 0}\frac{\mathrm{d}\theta}{\mathrm{d}s} = -\infty. \tag{A 10}$$

Since $(\mathrm{d}\theta/\mathrm{d}s) \leqslant 0$ on the curve AB and, according to the assumptions of the theorem, is finite, the infinite negative curvature of the free streamline AI gives rise to the flow region as in figure 3(*b*), which is two-sheeted in the neighbourhood of the point A.

Now let the curve AB be concave and $(\mathrm{d}\theta/\mathrm{d}s) \geqslant 0$. As follows from (A 8),

$$\omega'(0) = \theta'(0) = -\frac{2}{\pi}\int_0^\pi \theta'(\gamma)\sin\gamma\,\mathrm{d}\gamma. \tag{A 11}$$

From (A 4) we infer that $\theta'(\gamma) \leqslant 0$ and does not vanish identically. Hence $\omega'(0) > 0$.

If we consider separately the upper and lower parts of the parabola which the free streamlines approach, then according to Gilbarg (1960, p. 176)

$$y = \mp\omega'(0)\sqrt{\varphi_0 x}, \tag{A 12}$$

where $-$ and $+$ correspond to the upper and lower free streamlines respectively. This means that the upper and lower free streamlines overlap because $\omega'(0) > 0$. So the flow domain is two-sheeted in the neighbourhood of infinity. The theorem is proved.

REFERENCES

BIRKHOFF, G. & ZARANTONELLO, E. 1957 *Jets, Wakes and Cavities*. Academic.

BRILLOUIN, M. 1911 Les surfaces de glissement de Helmholtz et la resistance des fluides. *Ann. Chemie et Phys.* **23**, 145–230.

ELIZAROV, A. M., KASIMOV, A. R & MAKLAKOV, D. V. 2008 *Problems of Shape Optimization in Aerohydrodynamics*. Fizmatlit, in Russian.

FRANC, J.-P. & MICHEL, J.-M. 2004 *Fundamentals of Cavitation*. *Fluid Mechanics and its Applications, vol. 76*, Kluwer Academic.

GILBARG, D. 1960 *Jets, Wakes and Cavities*, *Encyclopedia of Physics, vol. 9*, pp. 311–445. Springer.

GOLUBEV, V. V. 1949 Lectures on wing theory. *Moscow, Gostekhizdat* (in Russian).

GUREVICH, M. I. 1966 *The Theory of Jets in an Ideal Fluid*. Pergamon.

LAVRENTIEV, M. 1938 Sur certaines propriétés des fonctions univalentes et leurs applications à la théorie des sillages. *Mat. Sbornik* **46**, 391–458.

LEVI-CIVITA, T. 1907 Scie e leggi di resistenza. *Rendeconti del Circolo Matematico di Palermo* **23**, 1–37.

MAKLAKOV, D. V. 1988 The maximum resistance of a curvilinear obstacle subjected to the action of free jets with separation. *Sov. Phys., Dokl.* **33** (1), 11–13. Translation from 1988 *Dokl. Akad. Nauk SSSR* **298** (3), 574–577.

MAKLAKOV, D. V. 1997 Nonlinear problems of hydrodynamics of potential flows with unknown boundaries. *Yanus-K. (in Russian)*.

MAKLAKOV, D. V. 1999 A note on the optimum profile of a sprayless planing surface. *J. Fluid Mech.* **384**, 281–292.

MAKLAKOV, D. V. 2004 Some remarks on the exact solution for an optimal impermeable parachute problem. *J. Comput. Appl. Math.* **166** (2), 591–596.

MAKLAKOV, D. V. 2005 On deflectors of optimum shape. *J. Fluid Mech.* **540**, 175–187.

MAKLAKOV, D. V., ELIZAROV, A. M. & SHARIPOV, R. R. 2007 On parachutes of optimum shape in a subsonic gas flow. *Eur. J. Appl. Math.* **18**, 81–102.

MAKLAKOV, D. V. & UGLOV, A. N. 1995 On the maximum drag of a curved plate in flow with a wake. *Eur. J. Appl. Math.* **6** (5), 517–527.

MILNE-THOMSON, L. M. 1962 *Theoretical Hydrodynamics*, 4th edition. Macmillan.

TAYLOR, G. I. 1926 Note on the connection between the lift of an aërofoil in a wind and the circulation round it. *Phil. Trans. R. Soc. Lond.* A **225**, 238–245. Appendix to the paper by Bryant, L.W. & Williams, D.H., An nvestigation of the flow of air around an aërofoil of infinite span.

WU, T. Y. 1972 Cavity and wake flows. *Annu. Rev. Fluid Mech.* **4**, 243–284.

WU, T. Y. & WHITNEY, A. K. 1972 Theory of optimum shapes in free-surface flows. Part 1. Optimum profile of sprayless planing surface. *J. Fluid Mech.* **55**, 439–455.